



Hydrophobic intensification flotation: Comparison of collector containing two minerophilic groups with conventional collectors

Sheng LIU, Guang-yi LIU, Yao-guo HUANG, Hong ZHONG

School of Chemistry and Chemical Engineering, Central South University, Changsha 410083, China

Received 6 January 2020; accepted 9 May 2020

Abstract: The surface hydrophobization and flotation of a xanthate–hydroxamate collector toward copper oxide mineral were compared with the combined collectors of xanthate and hydroxamate through water contact angle (WCA) and micro-flotation experiments. The results showed that S-[(2-hydroxyamino)-2-oxoethyl]-O-octyl-dithiocarbonate ester (HAOODE) exhibited stronger hydrophobization and better flotation performance to malachite ($\text{Cu}_2(\text{OH})_2\text{CO}_3$) than octyl-hydroxamic acid (OHA) and its combination with S-allyl-O-ethyl xanthate ester (AEXE). To understand the hydrophobic intensification mechanism of HAOODE to malachite, zeta potential, atomic force microscopy (AFM) and XPS measurements were carried out. The results recommended that malachite chemisorbed HAOODE to form Cu–HAOODE complexes in which the hydroxamate–(O,O)–Cu and –O–C(–S–Cu)–S– configurations co-existed. The co-adsorption of HAOODE’s hetero-difunctional groups was more stable than the single-functional-group adsorption of OHA and AEXE, which produced the “loop” structure and intensified the self-assembly alignment of HAOODE on malachite surfaces. In addition, the “h” shape steric orientation of the double hydrophobic groups in HAOODE facilitated stronger hydrophobization toward malachite than the “line” or “V” hydrophobic carbon chains of OHA or AEXE. Thus, HAOODE achieved the preferable flotation recovery of malachite particles in comparison with OHA and AEXE.

Key words: S-[(2-hydroxyamino)-2-oxoethyl]-O-octyl-dithiocarbonate ester; atomic force microscopy (AFM); hetero-difunctional co-adsorption; hydrophobization; malachite flotation

1 Introduction

Surface modification has a wide range of the technological and industrial applications in the anticorrosion [1], biosensors [2], nano-fabrication [3], and froth flotation [4,5]. In the flotation process, the surface hydrophobicity of valuable minerals is improved by the selective adsorption of surfactants, thus, these minerals can more easily attach gas bubbles to be floated out from their pulp [6].

Organic surfactants such as thiols [7], carboxylic acids [8], phosphonic acids [9,10], sulfonic acids [11], and hydroxamic acids [12] have

been widely used in froth flotation to enhance the surface hydrophobicity of transition metal minerals. For example, carboxylic acids are common surfactants used in beneficiation of non-sulfide minerals by formation of hydrophobic layers on mineral surfaces. Compared to carboxylic acids, hydroxamic acids exhibit strong affinity to transition-metal-containing minerals and good selectivity against Ca/Mg-containing minerals [13]. Therefore, hydroxamic acids have been considered as effective collectors for separation and recovery of Cu oxide minerals [14,15], and they anchor onto the surfaces of Cu oxide minerals mainly via generating the five-membered chelating rings with copper atoms [16]. Xanthates chemisorb on to

copper minerals surfaces through forming Cu—S bonds [17], they are traditional collectors for beneficiation of copper oxide or sulfide minerals.

Malachite with a chemical formula of $\text{Cu}_2\text{CO}_3(\text{OH})_2$ is an essential constituent of copper resources and exhibits the hydration and hydrophilicity in water. To enrich malachite by flotation technology, its surface hydrophobicity needs to be improved by surfactant modification. It is known that xanthates and hydroxamates can effectively hydrophobize malachite surfaces [18,19]. While, xanthates prefer to the surface-presulfidized malachite [20]. Nevertheless, in the presence of hydroxamates, xanthates exhibited the preferable flotation efficiency for recovery of malachite [21]. Thus, it is of interest to investigate malachite floatability by using novel surfactants containing both dithiocarbonate and hydroxamate groups. And the understanding of their hydrophobization mechanism can be deeply explored through comparison with that of single-polar-group collector, which is instructive in developing new flotation reagents.

In this work, a surfactant S-[(2-hydroxyamino)-2-oxoethyl]-O-octyl-dithiocarbonate ester (HAODE) was introduced as a flotation collector in beneficiation of malachite. The role of its dithiocarbonate and hydroxamate groups in interaction with malachite surfaces would be analyzed through zeta potential, AFM and XPS. And its hydrophobic flotation characteristics would be compared with those of the single-functional-group collectors including octyl-hydroxamic acid (OHA) and S-allyl-O-ethyl xanthate ester (AEXE) via water contact angle (WCA) and micro-flotation experiments.

2 Experimental

2.1 Materials

HAODE, OHA and AEXE were prepared following the reported approaches [22–24], and their chemical structures are shown in Fig. 1.

Other chemicals of analytical grade were used without further purification. Milli-Q water was used in AFM measurements and in other experiments, distilled water was adopted. The chunk mineral of malachite, quartz or calcite was sequentially processed by crushing, grinding and screening. The fraction with the particle size of 38–76 μm was

collected for micro-flotation and its specific surface area (SSA) was detected through Brunauer–Emmett–Teller (B.E.T) approach on Quantachrome Nova-1000 surface area analyzer (USA) [6,25]. The $-5 \mu\text{m}$ malachite particles were adopted in the XPS and zeta potential tests. The chemical compositions, XRD spectra, and SSAs of three minerals were reported in our previous studies [6,25]. The polishing and preparation procedures of malachite slices for AFM and WCA measurements were same as our previous investigations [26].

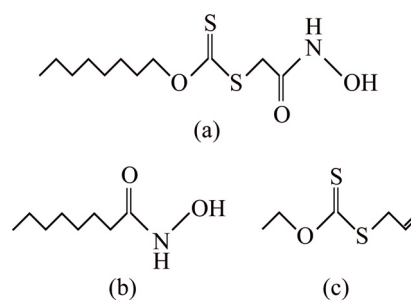


Fig. 1 Chemical structures of HAODE (a), OHA (b) and AEXE (c)

2.2 Contact angle and micro-flotation experiments

The water contact angle (WCA) and micro-flotation experiments were conducted in line with our previous approaches [26]. The static WCA was measured through the sessile drop method [27]. The presented WCA was the average value of four independent measurements on two different areas of a mineral surface. The recovery was calculated according to Eq. (1) for pure mineral, and Eqs. (2) and (3) for mineral in the artificially mixed minerals, respectively:

$$\varepsilon = \frac{m_1}{m_1 + m_2} \times 100\% \quad (1)$$

$$\varepsilon_{\text{Malachite}} = \frac{m_1 \alpha_1}{m_1 \alpha_1 + m_2 \alpha_2} \times 100\% \quad (2)$$

$$\varepsilon_{\text{Calcite/Quartz}} = \frac{m_1(1 - \alpha_1)}{m_1(1 - \alpha_1) + m_2(1 - \alpha_2)} \times 100\% \quad (3)$$

where m and α are the mass and copper grade, the subscripts 1 and 2 identify the froth and underflow products, respectively. The presented flotation recovery was the average value of three independent tests.

2.3 Zeta potential and AFM measurements

The ζ -potential of malachite in the presence or

absence of HAOODE was recorded on Brookhaven ZetaPlus analyzer (USA) in accordance with the reported operation [6]. The morphologies of malachite surfaces before/after HAOODE treatment were characterized on Bruker Dimension Icon AFM (Bruker, USA) through PeakForce Tapping of ScanAsyst Mode. After recording the AFM images of freshly-polished malachite, the malachite slice was soaked in 5×10^{-6} mol/L HAOODE solution, washed with Milli-Q water, dried by N_2 flow and its AFM images were then re-measured.

2.4 XPS measurements

The survey and high-resolution XPS of HAOODE, malachite and HAOODE-treated malachite were recorded on an ESCALAB 250Xi XPS (Thermo Fisher Scientific, USA) [6] under the pressure of the vacuum chamber less than 1.5×10^{-6} Pa. The XPS binding energy was calibrated by setting the C 1s binding energy at 284.80 eV. And the high-resolution XPS adsorption bands for N, O, S and Cu were fitted by the Thermo Avantage software [6]. The detailed processes for preparing were described as follows: 50 mg of malachite particles ($<5 \mu\text{m}$) were put into 300 mL of 1.0×10^{-4} mol/L HAOODE solution in a 500 mL conical flask. After stirring the suspension at 25°C for 4 h in a constant temperature shaker bath, malachite particles were filtered, washed thoroughly with distilled water, dried in a silica gel desiccator under vacuum for 3 d. The HAOODE and malachite with or without HAOODE treatment were pressed into a disk on a double-sided conductive adhesive carbon tape for XPS detection [22].

3 Results

3.1 Wettability

Figure 2(a) presented the influence of collector dose on the WCA of malachite. As seen from Fig. 2(a), after 1.50×10^{-5} mol/L OHA, OHA + AEXE (1.50×10^{-5} mol/L OHA + 1.50×10^{-5} mol/L AEXE) or HAOODE treatment for 5 min at pH 9.7, the WCA of malachite increased from $\sim 47.5^\circ$ to $\sim 94.5^\circ$, $\sim 96.5^\circ$ or $\sim 110.0^\circ$, respectively. The influence of pH on malachite's WCA was shown in Fig. 2(b). It displayed that under pH 6.0–10.5, HAOODE provided the higher malachite WCA than OHA and OHA+AEXE. Therefore, Fig. 2

demonstrated that HAOODE possessed stronger hydrophobization toward malachite than OHA and its combination with AEXE.

3.2 Micro-flotation

3.2.1 Single mineral flotation

Under 1.50×10^{-5} mol/L HAOODE, OHA or OHA + AEXE (1.50×10^{-5} mol/L AEXE), the flotation responses of malachite, calcite or quartz to pH were shown in Figs. 3(a–c). As observed from Figs. 3(a–c), flotation recovery of malachite reached around 83.7% for OHA and 85.2% for OHA+AEXE at their preferable pH ~ 9.7 . And, HAOODE enriched over 89.8% malachite particles in pH range of 7.5–10.5. While, the flotation recoveries of calcite and quartz were respectively below 35.0% and 20.0% by using any of the three collectors at $\text{pH} > 7.5$.

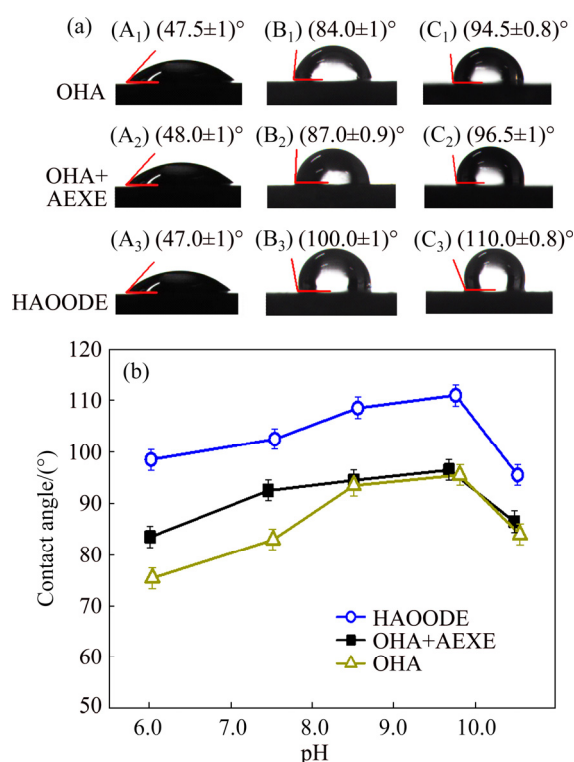


Fig. 2 WCA of malachite surfaces without/with collector immersion for 5 min at $\text{pH } 9.7 \pm 0.1$ (a) and as function of pH at 1.50×10^{-5} mol/L collector(s) (b) (A₁, B₁, C₁—0 mol/L; A₂, B₂, C₂— 1.00×10^{-5} mol/L; A₃, B₃, C₃— 1.50×10^{-5} mol/L)

Figures 3(d–f) displayed the relationship of collector concentration with the flotation recovery of malachite, calcite and quartz at pH around 9.7. It was elucidated that with increasing the collector concentration, the malachite recovery was increased

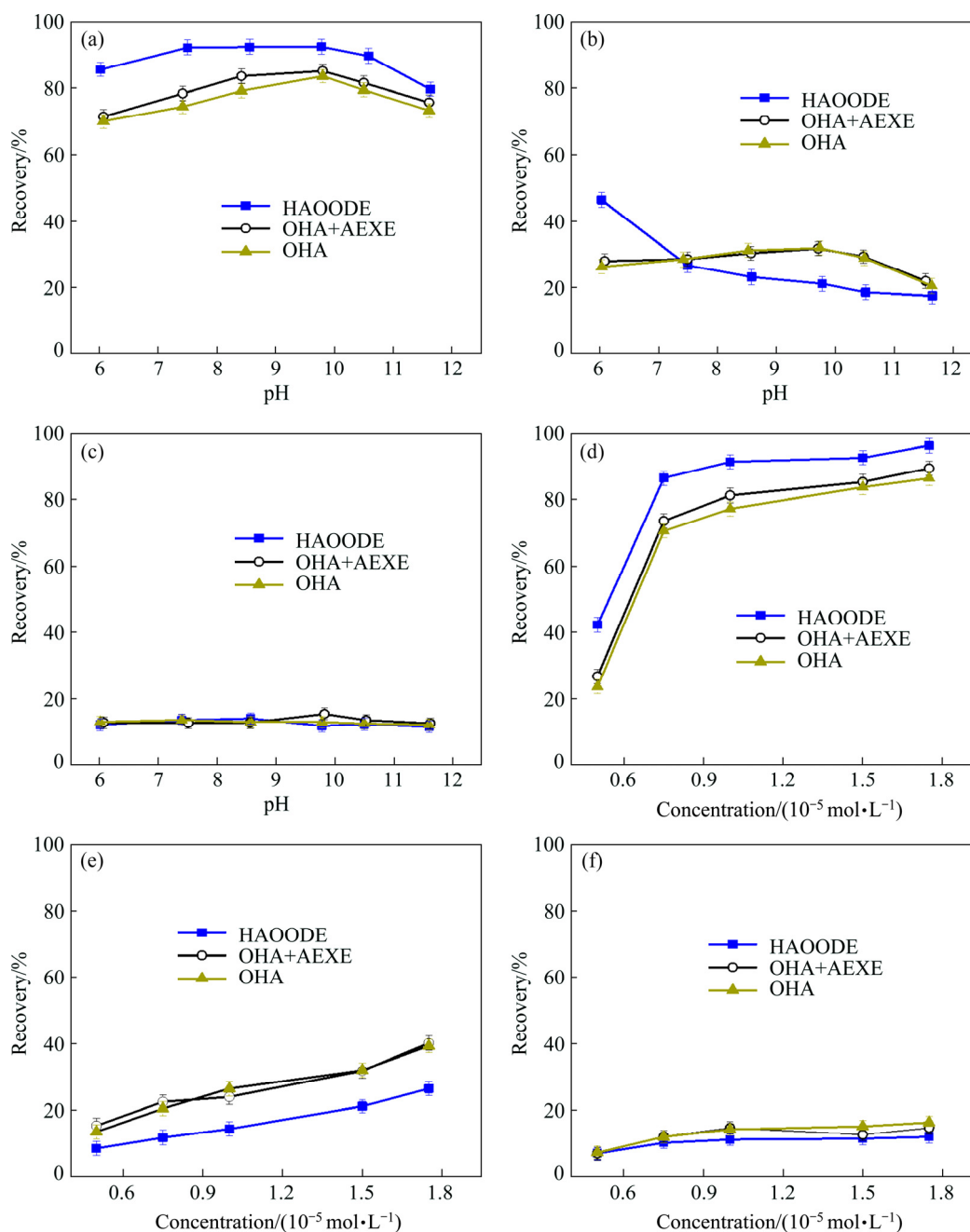


Fig. 3 Flotation recovery of malachite (a, d), calcite (b, e) and quartz (c, f) as function of pH at 1.50×10^{-5} mol/L collector(s) (a–c) and as function of collector concentration at pH 9.7 ± 0.1 (d–f)

rapidly, and 7.50×10^{-6} mol/L HAOODE, OHA and OHA+AEXE (7.50×10^{-6} mol/L AEXE) returned 86.4%, 70.6% and 73.6% malachite recovery, respectively. Subsequently, the malachite recovery increased gently with further increasing the collector concentration. Figures 3(d–f) also showed that HAOODE, OHA and OHA+AEXE possessed a good flotation selectivity against calcite and quartz. And among the three collectors, HAOODE exhibited the weakest collecting power toward calcite. Therefore, in comparison with OHA

and OHA+AEXE, HAOODE exhibited the preferable flotation characteristics for recovering malachite versus quartz and calcite from pH 7.5 to 10.5.

3.2.2 Separation of malachite from its artificial mixture with calcite or quartz

The flotation separation results of malachite from its mixture with calcite or quartz (the mass ratio of malachite to calcite or quartz was 1:1) with HAOODE collector were presented in Fig. 4. Figure 4(a) demonstrated that at 1.50×10^{-5} mol/L

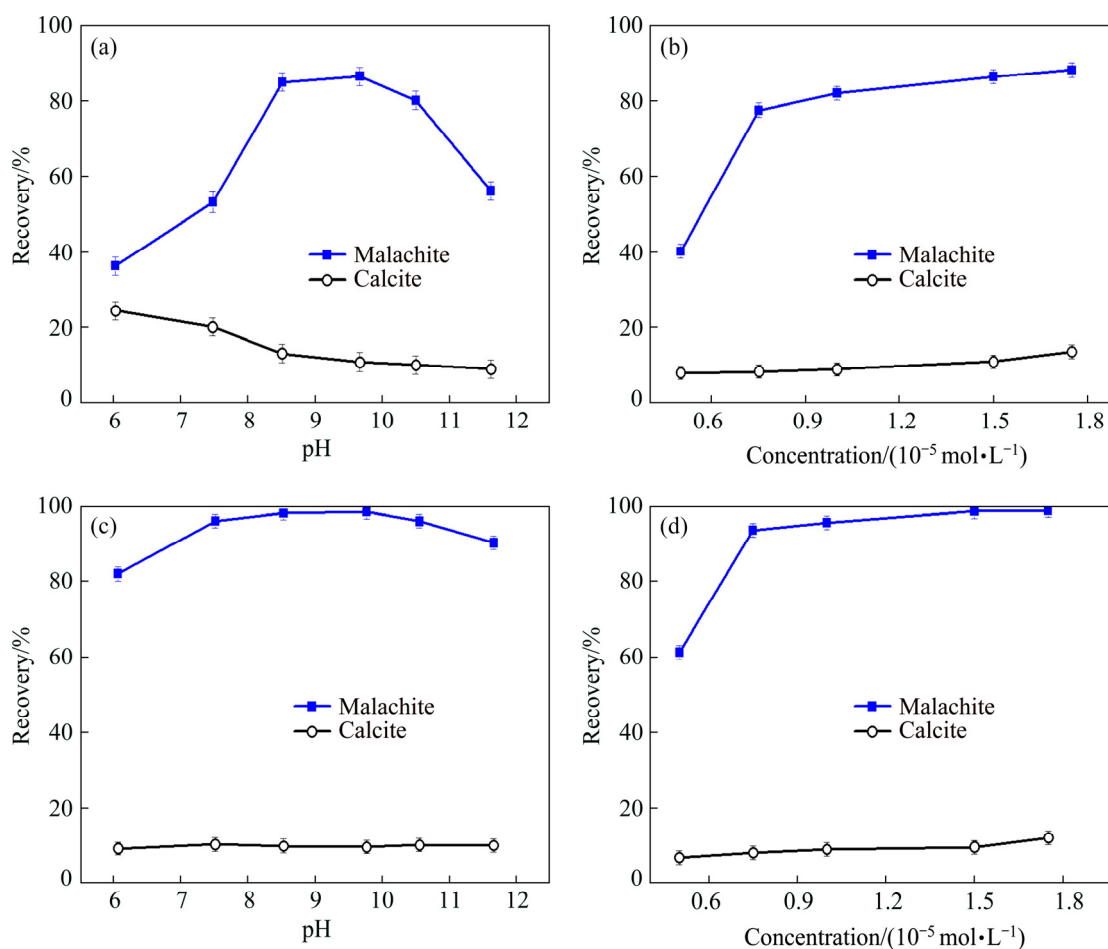


Fig. 4 Flotation results of artificially mixed minerals as function of pH at 1.50×10^{-5} mol/L HAOODE (a, c) and as function of initial HAOODE concentration at pH 9.7 ± 0.1 (b, d)

HAOODE, the preferred pH values for beneficiation of malachite from its mixture with calcite were 8.5–10.5 where more than 80.0% malachite particles were floated out with less than 15.0% calcite particles. Figure 4(b) indicated that at pH ~ 9.7 , HAOODE exhibited a good selectivity for flotation enrichment of malachite, especially under its concentration ranging from 7.50×10^{-6} to 1.75×10^{-5} mol/L.

Comparing the flotation results in Figs. 4(a) and (b) with those in Fig. 3, it was easy to conclude that in the presence of calcite, the floatability of malachite decreased, especially at $\text{pH} < 8.5$ or $\text{pH} > 10.5$, which might be caused by the competitive adsorption of malachite and calcite to HAOODE at $\text{pH} < 8.5$, or the cover effect of $\text{Ca}(\text{OH})^+$ species on malachite particles at $\text{pH} > 10.5$ [28].

Figures 4(c) and (d) showed the flotation results of malachite and quartz from their mixtures, which showed that HAOODE held an excellent

flotation selectivity to malachite against quartz under pH 6.0–11.6. In contrast to the flotation results displayed in Fig. 3, in the presence of quartz, malachite still maintained an admirable floatability, and at pH around 9.7, 1.75×10^{-5} mol/L HAOODE floated out 99.0% malachite and 12.1% quartz from their mixtures. Thus, quartz had an insignificant influence on malachite flotation.

3.3 Zeta potential

The ζ -potential of fine malachite particles in the presence and absence of 8.0×10^{-5} mol/L HAOODE was shown in Fig. 5. As observed from Fig. 5, the isoelectric point (IEP) of malachite occurred at pH about 8.7, near to the reported values [29]. In the presence of HAOODE, the IEP of malachite moved to lower pH at about 7.4, which might be owed to the anchor of HAOODE species with the surface copper sites on malachite.

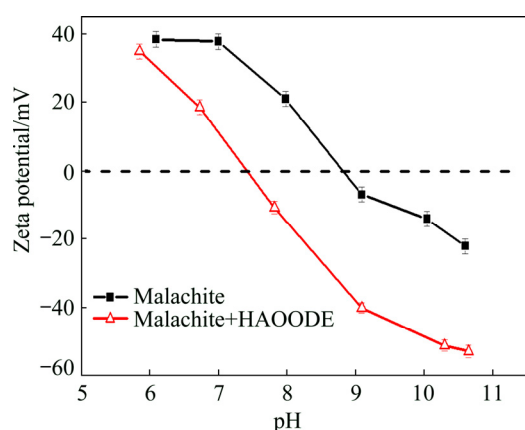


Fig. 5 Effect of pH on ζ -potential of malachite in the absence and presence of HAOODE

3.4 AFM results

The morphologies of malachite surfaces with or without HAOODE modification were illustrated in Fig. 6. The newly-polished malachite surfaces displayed a smooth appearance with 0.35 nm root-mean-square (RMS) roughness despite showing distinct scratches. After immersing in 5×10^{-6} mol/L HAOODE solution for 5 min, the whole malachite surfaces featured plenty of small aggregates with a RMS roughness increasing to 0.83 nm, and the previous scratches dramatically weakened. With extending the immersing time to 30 min, the roughness of malachite surfaces significantly increased to 2.06 nm RMS, and the scratches originated from polishing operation were invisible. Therefore, AFM images clearly demonstrated that HAOODE aggregated on the whole malachite surfaces, which was the reason why HAOODE realized the surface hydrophobization and flotation recovery of malachite particles.

3.5 XPS spectra

3.5.1 Survey XPS

The XPS-detected elements and their atomic compositions of HAOODE, malachite, and HAOODE-modified malachite were shown in Fig. 7 and Table 1. As illustrated from Fig. 7 and Table 1, the mole ratio of C to O to S and to N for HAOODE was measured to be about 11:3:2:1, which was in good agreement with its molecular formula of $C_{11}H_{22}O_3S_2N$ except the undetected H. And the mole ratio of copper to HAOODE in Cu-HAOODE compounds was 1:1 [22]. As we have known, the chelating proportion of cupric ion to hydroxamate group is 1:2 in their five-membered

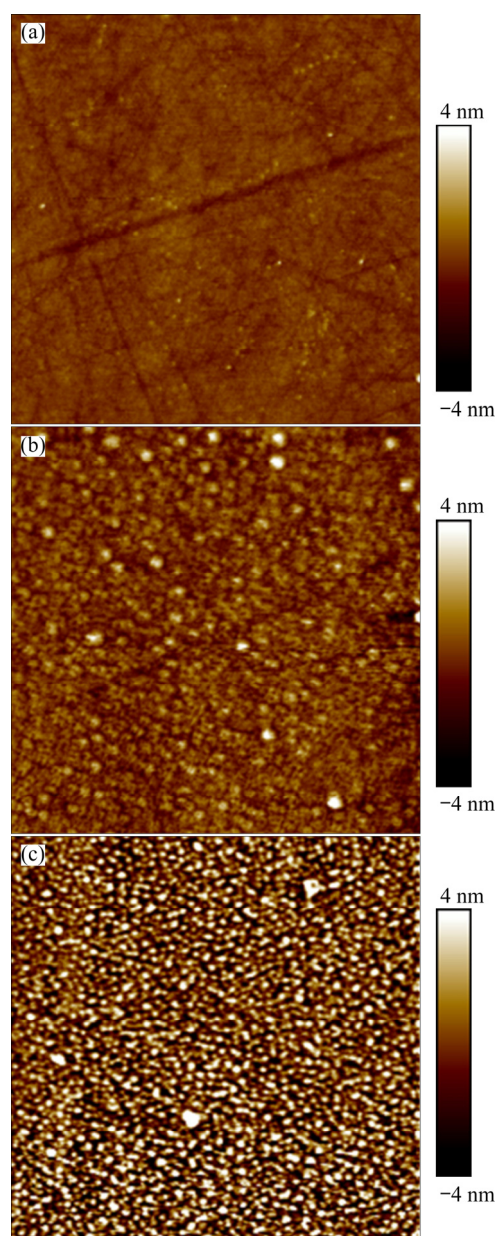


Fig. 6 AFM topographic images ($5 \mu\text{m} \times 5 \mu\text{m}$) of newly-polished malachite surface (a) and after HAOODE treatment for 5 min (b) and 30 min (c)

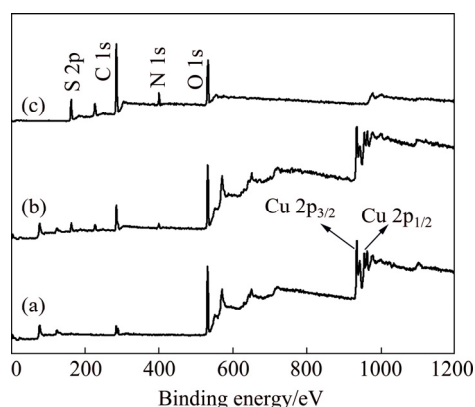


Fig. 7 XPS survey spectra of malachite before (a) and after treatment of HAOODE (b) and HAOODE (c)

hydroxamate—(O,O)—Cu(O—Cu(II)—O—N=C—) structure [23]. Thus, besides —C(=O)—NH—OH, the C(=S)—S— group might attend the bonding interaction with copper atom(s) in the Cu—HAOODE complexes [22]. For HAOODE-modified malachite, the appearing sulfur and nitrogen XPS peaks meant that HAOODE anchored on malachite surfaces.

3.5.2 High-resolution XPS

Figure 8 (S 2p) and Table 2 (S 2p) displayed that the S 2p_{3/2} XPS bands [6] of HAOODE were composed of two nearly equal compositions separately at about 161.92 and 163.36 eV, which were attributed to the S atoms in the C=S and C—S—C groups [30], respectively. After HAOODE adsorption on malachite, the XPS band of S related to C=S shifted from 161.92 to 162.58 eV [22], which inferred the electron donation of thiocarbonyl S atom to surface copper atom(s) with forming Cu—S bond(s) on malachite [30]. Meanwhile, the thioether S further delocalized its electron(s) to the —O—C(=S)—S— group to compensate the electron loss of thiocarbonyl S atom, leading to its binding energy increasing from 163.36 to 163.85 eV [22].

As observed from Fig. 8(N 1s) and Table 2 (N 1s), the N 1s XPS of HAOODE appeared at about 400.29 eV. After HAOODE interaction, the N 1s peak arose at around 399.84 eV on malachite, which was very close to that at about 399.93 eV for Cu—HAOODE precipitates [22]. Figure 8(O 1s) and Table 2 (O 1s) showed that the O 1s XPS bands of HAOODE included three compositions with similar peak area, being assigned to the O atoms of OH (530.83 eV) [31], C=O (532.43 eV) [32] and C—O—C (533.00 eV) groups, respectively. For the Cu—HAOODE complex [22], its O 1s XPS bands contained two characteristic peaks at about 532.00 and 533.30 eV, being attributed to the two O atoms in —C(O⁻)=N—O⁻ group [32] and the ether O atom in C—O—C(—S)—S— group [33,35], respectively.

Figure 8(Cu 2p) and Table 2 (Cu 2p) elucidated that Cu 2p_{3/2} binding energy of malachite was about 934.88 eV, being identical to cupric oxide species [6,36]. After HAOODE treatment, the Cu 2p_{3/2} XPS bands of malachite changed into two Gaussian–Lorentzian compositions at about 934.92 and 932.89 eV, respectively, with proportions of 59.52% and 40.48%, which were identical to Cu(II)

Table 1 Mole fraction of elements as determined by XPS

Species	Mole fraction/%					Mole fraction ratio to Cu/%				
	C 1s	N 1s	O 1s	S 2p	Cu 2p	C 1s	N 1s	O 1s	S 2p	Cu 2p
HAOODE	65.43	5.91	17.16	11.50	—	—	—	—	—	—
Malachite [6]	26.32	0.40	49.78	—	23.50	1.12	0.02	2.12	—	1.00
Malachite treated by HAOODE	41.94	3.18	33.21	6.59	15.09	2.78	0.21	2.20	0.44	1.00

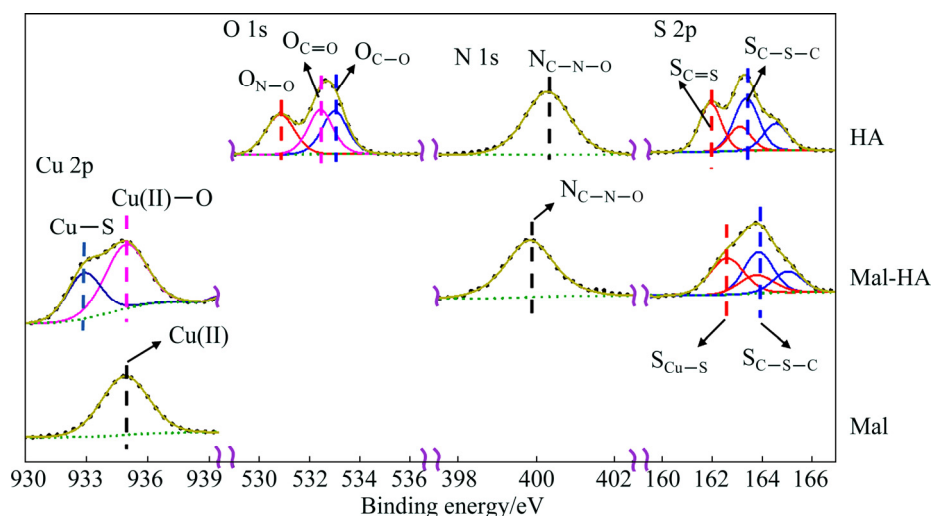


Fig. 8 XPS spectra of Cu 2p_{3/2}, O 1s, N 1s and S 2p (HAOODE(HA), malachite (Mal) before/after HAOODE adsorption)

Table 2 Results of deconvolution with Gaussian–Lorentzian bands of S 2p, N 1s, O 1s and Cu 2p

Band	Species	Binding energy/eV	FWHM ^a /eV	Mole fraction/%	Assignment
S 2p	HAOODE	161.92/163.10 ^b	1.08/1.08	36.36/18.55	S _{C-S} [22,30]
		163.36/164.54 ^b	1.22/1.22	29.82/15.27	S _{C-S-C} [22,30]
	Malachite adsorbed HAOODE	162.58/163.76 ^b	1.70/1.70	33.67/17.17	S _{S-Cu} [30]
		163.85/165.03 ^b	1.44/1.44	32.66/16.50	S _{C-S-C} [22,30]
N 1s	HAOODE	400.29	1.43	100.00	N _{C-N-O} [30]
	Malachite adsorbed HAOODE	399.84	1.52	100.00	N _{C-N-O} [22]
O 1s	HAOODE	530.83	1.42	34.01	O _{N-O} [31]
		532.43	1.22	33.33	O _{C=O} [32]
		533.00	1.24	32.66	O _{C-O} [33]
Cu 2p	Malachite [6]	934.88	2.83	100.00	Cu(II) [6]
	Malachite treated by HAOODE	932.89	2.06	40.48	Cu(I)—S [34]
		934.92	2.50	59.52	Cu(II)—O [6]

^aFWHM: Full width of half maximum; ^b(S 2p_{3/2})/(S 2p_{1/2})

oxide [6] and Cu sulfide species [34]. This implied the bonding interaction of interface Cu(II) on malachite with both hydroxamate and dithiocarbonate groups of HAOODE, being consistent to the interaction of HAOODE with cupric ion [22]. By comparing the Cu 2p, S 2p and N 1s XPS peaks of HAOODE-treated malachite with those of Cu—HAOODE complexes, it was easy to conclude that malachite chemisorbed HAOODE via forming Cu—HAOODE complexes.

4 Discussion

HAOODE exhibited stronger hydrophobization toward malachite than OHA and OHA+AEEXE, and it also achieved higher flotation recovery of malachite than OHA and OHA+AEEXE at pH 6.0–10.5. AFM images clearly showed that HAOODE aggregated on the whole surface of malachite, which realized the surface hydrophobization and flotation recovery of malachite particles. The existence of HAOODE led to a negative move of malachite's ζ -potential at pH 6.5–10.6. At pH > 9.5, malachite particles were negatively charged (see Fig. 5) and the —C(=O)—NH—OH of HAOODE was ionized to —C(=O)—NH—O⁻ anion [37]. Nevertheless, HAOODE anions did adsorb onto malachite surfaces (see Fig. 5), implying that there existed a strong chemisorption between them enough to overcome their electrostatic repulsion [38]. It

was easy to conclude from the XPS observation that malachite adsorbed HAOODE via forming Cu—HAOODE complexes in which the five-membered hydroxamate—(O,O)—Cu(O—Cu(II)—O—N=C—) and —O—C(—S—Cu)—S— configurations co-existed [32,39].

Based on the findings and discussion mentioned above, a potential self-assembly model of HAOODE on the malachite surfaces was proposed as presented in Fig. 9(a). HAOODE self-assembled on malachite surfaces by bonding surface copper atoms through both —O—C(=S)—S— and —C(=O)—NH—OH groups to build Cu—S and O—Cu(II)—O bonds. For the hydroxamate —(O,O)—Cu configuration, its valence electrons could readily delocalize in the five-membered ring, leading to an increasing electron density around its N atom thus to lower the N 1s binding energy as shown in Fig. 8(N 1s) and Table 2(N 1s). In the —O—C(—S—Cu)—S— structure, the S atom of C=S group in HAOODE molecule donated its valence electrons to Cu atom to form Cu—S bond(s). To compensate the withdrawal of electrons from —O—C(=S)—S— group, the ether O and thioether S atoms contributed part electron(s) to the C—S—Cu group, causing increasing O 1s and S 2p binding energies of the ether O and thioether S atoms in the —O—C(—S—Cu)—S— group. As a comparison, the adsorption models of OHA or OHA+AEEXE on malachite surfaces were also recommended and

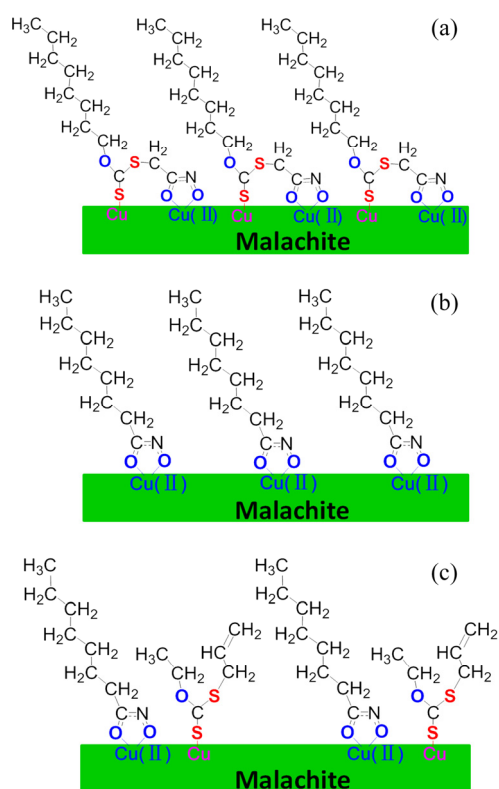


Fig. 9 Potential hydrophobicity model of HAOODE (a), OHA (b) and OHA+AEXE (c) on malachite surfaces

presented in Figs. 9(b) and (c) [40,41].

In contrast with a single-functional-group chelator, a difunctional group molecule commonly forms preferably stable complexes with metal atoms [16,42]. Thus, the hetero-difunctional-group HAOODE should generate more stable Cu complexes on malachite surfaces than the single-functional-group OHA and AEXE. Furthermore, the $-\text{O}-\text{C}(=\text{S})-\text{S}-$ and $-\text{C}(=\text{O})-\text{NH}-\text{OH}$ groups in HAOODE molecule are connected through the $-\text{CH}_2-$ group which is stable enough to conquer the potential repulsive interaction between the two hetero-difunctional groups during HAOODE approach to malachite. As a result, HAOODE might align closer on malachite surfaces than OHA and OHA+AEXE as shown in Fig. 9 [43,44]. Figure 9(c) showed that the co-adsorption of AEXE with OHA decreased the hydrated region of malachite surfaces, while the steric hindrance between their hydrophobic carbon chains would weaken their close alignment. In addition, the co-adsorption of HAOODE's hetero-difunctional groups formed the "loop" structure on malachite surfaces [6], which caused the "h" shape steric orientation of HAOODE's double

hydrophobic groups to display stronger hydrophobization toward malachite than the "line" or "V" hydrophobic carbon chains of OHA or AEXE. Therefore, HAOODE achieved the preferable flotation recovery of malachite particles in comparison with OHA and AEXE.

5 Conclusions

(1) The hydrophobization of HAOODE toward malachite was stronger than that of OHA and OHA+AEXE. And HAOODE achieved higher flotation recovery of malachite than OHA and OHA+AEXE at pH 6.0–10.5.

(2) AFM images clearly demonstrated that HAOODE aggregated on the whole surface of malachite, which realized the surface hydrophobization and flotation recovery of malachite particles. The existence of HAOODE led to a negative move of malachite's ζ -potential at pH 6.5–10.6. XPS recommended that malachite chemisorbed HAOODE to form Cu—HAOODE complexes in which the hydroxamate—(O,O)—Cu(O—Cu(II)—O—N=C—) and —O—C(—S—Cu)—S— configurations co-existed.

(3) The co-adsorption of HAOODE's hetero-difunctional groups on to malachite was more stable than the single-functional-group adsorption of OHA and AEXE, which produced the "loop" structure and intensified the self-assembly alignment of HAOODE on malachite surfaces. In addition, the "h" shape steric orientation of the double hydrophobic groups in HAOODE facilitated stronger hydrophobization toward malachite than the "line" or "V" hydrophobic carbon chains of OHA or AEXE. Thus, HAOODE achieved the preferable flotation recovery of malachite particles in comparison with OHA and AEXE.

References

- [1] ALAGTA A, FELHOSI I, BERTOTI I, KALMAN E. Corrosion protection properties of hydroxamic acid self-assembled monolayer on carbon steel [J]. Corrosion Science 2008, 50: 1644–1649.
- [2] DIAO Jian-pian, REN Da-cheng, ENGSTROM J R, LEE K H. A surface modification strategy on silicon nitride for developing biosensors [J]. Analytical Biochemistry, 2005, 343: 322–328.
- [3] YAH W O, TAKAHARA A, LVOV Y M. Selective modification of halloysite lumen with octadecylphosphonic acid: New inorganic tubular micelle [J]. Journal of the

- American Chemical Society, 2012, 134: 1853–1859.
- [4] ZHU Hai-ling, QIN Wen-qing, CHEN Chen, CHAI Li-yuan, LI Lai-shun, LIU San-jun, ZHANG Ting. Selective flotation of smithsonite, quartz and calcite using alkyl diamine ether as collector [J]. Transactions of Nonferrous Metals Society of China, 2018, 28: 163–168.
- [5] YIN Wan-zhong, SUN Qian-yu, LI Dong, TANG Yuan, FU Ya-feng, YAO Jin. Mechanism and application on sulphidizing flotation of copper oxide with combined collectors [J]. Transactions of Nonferrous Metals Society of China, 2019, 29: 178–185.
- [6] LIU Sheng, ZHONG Hong, LIU Guang-yi, XU Zheng-he. Cu(I)/Cu(II) mixed-valence surface complexes of S-[(2-hydroxyamino)-2-oxoethyl]-N,N-dibutylthiocarbamate: Hydrophobic mechanism to malachite flotation [J]. Journal of Colloid and Interface Science, 2018, 512: 701–712.
- [7] KHOSO S A, HU Yue-hua, LÜ Fei, GAO Ya, LIU Run-qing, SUN Wei. Xanthate interaction and flotation separation of H₂O₂-treated chalcopyrite and pyrite [J]. Transactions of Nonferrous Metals Society of China, 2019, 29: 2604–2614.
- [8] BAUER T, SCHMALTZ T, LENZ T, HALIK M, MEYER B, CLARK T. Phosphonate- and carboxylate-based self-assembled monolayers for organic devices: A theoretical study of surface binding on aluminum oxide with experimental support [J]. ACS Applied Materials & Interfaces, 2013, 5: 6073–6080.
- [9] XIAO Wei, REN Ya-xin, YANG Juan, CAO Pan, WANG Jun, QIN Wen-qing, QIU Guan-zhou. Adsorption mechanism of sodium oleate and styryl phosphonic acid on rutile and amphibole surfaces [J]. Transactions of Nonferrous Metals Society of China, 2019, 29: 1939–1947.
- [10] HUANG Xiao-tao, XIAO Wei, ZHAO Hong-bo, CAO Pan, HU Qi-xiu, QIN Wen-qing, ZHANG Yan-sheng, QIU Guan-zhou, WANG Jun. Hydrophobic flocculation flotation of rutile fines in presence of styryl phosphonic acid [J]. Transactions of Nonferrous Metals Society of China, 2018, 28: 1424–1432.
- [11] FIURASEK P, REVEN L. Phosphonic and sulfonic acid-functionalized gold nanoparticles: A solid-state NMR study [J]. Langmuir, 2007, 23: 2857–2866.
- [12] WANG Li, HU Guang-yan, KHOSO S A, LIU Run-qing, ZHANG Xiang-feng. Selective flotation of smithsonite from dolomite by using novel mixed collector system [J]. Transactions of Nonferrous Metals Society of China, 2019, 29: 1082–1089.
- [13] YUE Tong, HAN Hai-sheng, HU Yue-hua, SUN Wei, LI Xiao-dong, LIU Run-qing, GAO Zhi-yong, WANG Li, CHEN Pan, ZHANG Chen-yang. New insights into the role of Pb-BHA complexes in the flotation of tungsten minerals [J]. JOM, 2017, 69: 2345–2351.
- [14] FENG Qi-cheng, ZHAO Wen-juan, WEN Shu-ming, CAO Qin-bo. Activation mechanism of lead ions in cassiterite flotation with salicylhydroxamic acid as collector [J]. Separation and Purification Technology, 2017, 178: 193–199.
- [15] XU Hai-feng, ZHONG Hong, TANG Qing, WANG Shuai, ZHAO Gang, LIU Guang-yi. A novel collector 2-ethyl-2-hexenoic hydroxamic acid: Flotation performance and adsorption mechanism to ilmenite [J]. Applied Surface Science, 2015, 353: 882–889.
- [16] PUJARI S P, SCHERES L, MARCELIS A T, ZUILHOF H. Covalent surface modification of oxide surfaces [J]. Angewandte Chemie International Edition, 2014, 53: 6322–6356.
- [17] TZHAYIK O, SAWANT P, EFRIMA S, KOVALEV E, KLUG J. Xanthate capping of silver, copper, and gold colloids [J]. Langmuir, 2002, 18: 3364–3369.
- [18] LEE K, ARCHIBALD D, MCLEAN J, REUTER M A. Flotation of mixed copper oxide and sulphide minerals with xanthate and hydroxamate collectors [J]. Minerals Engineering, 2009, 22: 395–401.
- [19] MARION C, JORFENS A, LI R, RUDOLPH M, WATERS K E. An evaluation of hydroxamate collectors for malachite flotation [J]. Separation and Purification Technology, 2017, 183: 258–269.
- [20] PARK K, PARK S, CHOI J, KIM G, TONG M, KIM H. Influence of excess sulfide ions on the malachite-bubble interaction in the presence of thiol-collector [J]. Separation and Purification Technology, 2016, 168: 1–7.
- [21] LEE J, NAGARAJ D, COE J. Practical aspects of oxide copper recovery with alkyl hydroxamates [J]. Minerals Engineering, 1998, 11: 929–939.
- [22] LIU Sheng, XIE Lei, LIU Guang-yi, ZHONG Hong, WANG Yi-xiang, ZENG Hong-bo. Hetero-difunctional reagent with superior flotation performance to chalcopyrite and associated surface interaction mechanism [J]. Langmuir, 2019, 35: 4353–4363.
- [23] YANG Xiang-lin, LIU Sheng, LIU Guang-yi, ZHONG Hong. A DFT study on the structure-reactivity relationship of aliphatic oxime derivatives as copper chelating agents and malachite flotation collectors [J]. Journal of Industrial and Engineering Chemistry, 2017, 46: 404–415.
- [24] ZHOU Ji-liang. The preparation and application of three series of alkyl xanthate esters [D]. Changsha: Central South University, China, 2003. (in Chinese)
- [25] HUANG Yao-guo, NIU Xiao-xue, LIU Guang-yi, LIU Jun. Novel chelating surfactant 5-heptyl-1,2,4-triazole-3-thione: Its synthesis and flotation separation of malachite against quartz and calcite [J]. Minerals Engineering, 2019, 131: 342–352.
- [26] LIU Guang-yi, QIU Zhao-hui, WANG Jing-yi, LIU Qing-xia, XIAO Jing-jing, ZENG Hong-bo, ZHONG Hong, XU Zheng-he. Study of N-isopropoxypropyl-N'-ethoxycarbonyl thiourea adsorption on chalcopyrite using in situ SECM, ToF-SIMS and XPS [J]. Journal of Colloid and Interface Science, 2015, 437: 42–49.
- [27] SHI Feng, WANG Zhi-qiang, ZHANG Xi. Combining a layer-by-layer assembling technique with electrochemical deposition of gold aggregates to mimic the legs of water striders [J]. Advanced Materials, 2005, 17: 1005–1009.
- [28] SHI Qing, ZHANG Guo-fan, FENG Qi-ming, DENG Hong. Effect of solution chemistry on the flotation system of smithsonite and calcite [J]. International Journal of Mineral Processing, 2013, 119: 34–39.
- [29] CHOI J, CHOI S Q, PARK K, HAN Y, KIM H. Flotation behaviour of malachite in mono- and di-valent salt solutions using sodium oleate as a collector [J]. International Journal

- of Mineral Processing, 2016, 146: 38–45.
- [30] LIU Sheng, LIU Guang-yi, ZHONG Hong, YANG Xiang-lin. The role of HABTC's hydroxamate and dithiocarbamate groups in chalcopyrite flotation [J]. Journal of Industrial and Engineering Chemistry, 2017, 52: 359–368.
- [31] BIESINGER M C, PAYNE B P, LAU L W, GERSON A, SMART R S C. X-ray photoelectron spectroscopic chemical state quantification of mixed nickel metal, oxide and hydroxide systems [J]. Surface and Interface Analysis, 2009, 41: 324–332.
- [32] HOPE G A, WOODS R, PARKER G K, BUCKLEY A N, MCLEAN J. Spectroscopic characterisation of copper acetohydroxamate and copper n-octanohydroxamate [J]. Inorganica Chimica Acta, 2011, 365: 65–70.
- [33] LOPEZ G P, CASTNER D G, RATNER B D. XPS O 1s binding energies for polymers containing hydroxyl, ether, ketone and ester groups [J]. Surface and Interface Analysis, 1991, 17: 267–272.
- [34] FREEMAN T, EVANS S, ULMAN A. XPS studies of self-assembled multilayer films [J]. Langmuir, 1995, 11: 4411–4417.
- [35] KUNDU S, WANG Y, XIA W, MUHLER M. Thermal stability and reducibility of oxygen-containing functional groups on multiwalled carbon nanotube surfaces: A quantitative high-resolution XPS and TPD/TPR study [J]. The Journal of Physical Chemistry C, 2008, 112: 16869–16878.
- [36] LIU Guang-yi, HUANG Yao-guo, QU Xiao-yan, XIAO Jing-jing, YANG Xiang-lin, XU Zheng-he. Understanding the hydrophobic mechanism of 3-hexyl-4-amino-1,2,4-triazole-5-thione to malachite by ToF-SIMS, XPS, FTIR, contact angle, zeta potential and micro-flotation [J]. Colloids and Surfaces A: Physicochemical and Engineering Aspects, 2016, 503: 34–42.
- [37] PARKER G K, HOLT S A, HOPE G A. Characterisation of the deposition of n-octanohydroxamate on copper surfaces [J]. ECS Transactions, 2013, 50: 23–33.
- [38] LI Fang-xu, ZHONG Hong, ZHAO Gang, WANG Shuai, LIU Guang-yi. Flotation performances and adsorption mechanism of α -hydroxyoctyl phosphinic acid to cassiterite [J]. Applied Surface Science, 2015, 353: 856–864.
- [39] EDWARDS D C, MYNENI S C. Hard and soft X-ray absorption spectroscopic investigation of aqueous Fe(III)-hydroxamate siderophore complexes [J]. The Journal of Physical Chemistry A, 2005, 109: 10249–10256.
- [40] MA Xin, XIA Liu-yin, WANG Shuai, ZHONG Hong, JIA Hui. Structural modification of xanthate collectors to enhance the flotation selectivity of chalcopyrite [J]. Industrial & Engineering Chemistry Research, 2017, 56: 6307–6316.
- [41] HOPE G A, WOODS R, PARKER G K, BUCKLEY A N, MCLEAN J. A vibrational spectroscopy and XPS investigation of the interaction of hydroxamate reagents on copper oxide minerals [J]. Minerals Engineering, 2010, 23: 952–959.
- [42] DENAYER J, DELHALLE J, MEKHALIF Z. Self-assembly of amine terminated alkythiol and alkyldithiol films on a polycrystalline copper substrate [J]. Journal of Electrochemistry Society, 2011, 158: 100–108.
- [43] HUANG Zhi-qiang, ZHONG Hong, WANG Shuai, XIA Liu-yin, ZOU Wen-bo, LIU Guang-yi. Investigations on reverse cationic flotation of iron ore by using a Gemini surfactant: Ethane-1,2-bis (dimethyl-dodecyl-ammonium bromide) [J]. Chemical Engineering Journal, 2014, 257: 218–228.
- [44] DENG Lan-qing, ZHONG Hong, WANG Shuai, LIU Guang-yi. A novel surfactant N-(6-(hydroxyamino)-6-oxohexyl) octanamide: synthesis and flotation mechanisms to wolframite [J]. Separation and Purification Technology, 2015, 145: 8–16.

疏水强化浮选：双亲矿基捕收剂与常规捕收剂的对比

刘胜, 刘广义, 黄耀国, 钟宏

中南大学 化学化工学院, 长沙 410083

摘要: 通过接触角和单矿物浮选试验, 对比研究黄原酸酯-羟肟酸双配体捕收剂与黄原酸酯+羟肟酸组合捕收剂对氧化铜矿物浮选和疏水性能。结果表明, S-[(2-羟胺基)-2-乙酰基]-O-辛基-二硫代碳酸酯(HAOODE)对孔雀石的疏水化能力和浮选性能优于辛基羟肟酸(OHA)及其与 S-烯丙基-O-乙基黄原酸酯(AEXE)的组合。通过动电位测试、原子力显微镜扫描和 XPS 分析, 考察 HAOODE 对孔雀石的疏水强化机理。结果显示, HAOODE 化学吸附在孔雀石表面, 形成含羟肟酸-(O,O)-Cu 和 -O-C(-S-Cu)-S-构型的表面 Cu-HAOODE 络合物。HAOODE 的双官能团共吸附产生了“环”形结构, 比 OHA 和 AEXE 的单官能团吸附更稳定, 强化其在孔雀石表面的吸附。此外, 与 OHA 的“线”形和 AEXE 的“V”形疏水碳链相比, HAOODE 的“h”形双疏水基强化了孔雀石表面疏水。因此, 与 OHA 和 AEXE 相比, HAOODE 对孔雀石颗粒浮选回收率更高。

关键词: S-[(2-羟胺基)-2-乙酰基]-O-辛基-二硫代碳酸酯; 原子力显微镜扫描; 双官能团共吸附; 疏水; 孔雀石浮选

(Edited by Xiang-qun LI)